

Algebraic Methods in Mechanism Analysis and Synthesis

Manfred L. Husty, Martin Pfurner, Hans-Peter Schröcker,
Karin Brunthaler

University Innsbruck, Institute of Basic Sciences in Engineering, Unit Geometry and CAD
Technikerstraße 13, A6020 Innsbruck, Austria

email: `manfred.husty`, `martin.pfurner`, `hans-peter.schoecker`,
`katrin.brunthaler@uibk.ac.at`

Abstract: Algebraic methods in connection with classical multidimensional geometry have proven to be very efficient in the computation of direct and inverse kinematics of mechanisms as well as the explanation of strange, pathological behavior. In this paper we give an overview of the results achieved within the last years using the algebraic geometric method, geometric preprocessing and numerical analysis. We provide the mathematical and geometrical background, like Study's parametrization of the Euclidean motion group, the ideals belonging to mechanism constraints and methods to solve polynomial equations. The methods are explained with different examples from mechanism analysis and synthesis.

Keywords: Kinematic Mapping, constraint manifolds, mechanism analysis, mechanism synthesis, Bennett mechanism, 6R inverse kinematics, overconstrained mechanisms.

1 Introduction

There are many different mathematical methods in dealing with mechanism analysis and synthesis. Matrix and vector methods are most common to derive equations that describe the mechanisms (see e.g. Angeles [1]). Generally these methods have the disadvantage, that one has to deal with sines and cosines, which are eliminated using half tangent substitutions. Within the last ten years algebraic methods have become successful in solving problems in mechanism analysis and synthesis. One of the main reasons are the advances in solving systems of polynomial equations. Many algorithms have been developed, all of them heavily relying on the use of computer algebra systems (see e.g. Dickenstein et.al. [9]).

In mechanism science is important to find the simplest mathematical modeling of a mechanism, because the systems of equations describing the mechanisms generally are very complicated. Therefore it seems to be advantageous to have additionally a geometrical setting for the interpretation of the equations. Kinematic image spaces provide such a setting. They have been introduced by W. Blaschke [5] and E. Study [25] and have been forgotten for long time. The main contribution of this overview paper is to show that geometric preprocessing and an understanding of the multidimensional geometry of kinematic image spaces is crucial to find simple sets of equations, which then can be solved efficiently using all the advances in computer algebra and the newly introduced methods in polynomial equation solving.

The paper is organized as follows: In the remaining part of the introduction the mathematical background and the algebraic-geometric method to derive constraint equations for mechanism analysis and synthesis is provided. Section 2 gives then the application of the devised algorithms to mechanism analysis, especially the inverse kinematics of serial $6R$ -chains and the determination of the motion of overconstrained mechanisms. Section 3 deals with the synthesis of Bennett mechanisms.

1.1 Study-Model of SE(6)

Euclidean displacements $\mathcal{D} \in SE(6)$ can be described by (see [13, 19])

$$\mathcal{D}: \mathbf{x}' = \mathbf{A}\mathbf{x} + \mathbf{t}, \quad (1)$$

where \mathbf{x}' resp. \mathbf{x} represent a point in the fixed resp. moving frame, \mathbf{A} is a 3×3 proper orthogonal matrix and $\mathbf{t} = (t_1, t_2, t_3)^T$ is the translation vector, connecting the origins of moving and fixed frame. Expanding the dual quaternion representation (see [13, Section 3.3.2]) and using an operator approach, the matrix operator corresponding to the normalized dual quaternion $\mathbf{q} = (x_0, x_1, x_2, x_3)^T + \varepsilon(y_0, y_1, y_2, y_3)^T$ is given by

$$\mathbf{M} := \begin{bmatrix} 1 & 0 & 0 & 0 \\ t_1 & x_0^2 + x_1^2 - x_3^2 - x_2^2 & -2x_0x_3 + 2x_2x_1 & 2x_3x_1 + 2x_0x_2 \\ t_2 & 2x_2x_1 + 2x_0x_3 & x_0^2 + x_2^2 - x_1^2 - x_3^2 & -2x_0x_1 + 2x_3x_2 \\ t_3 & -2x_0x_2 + 2x_3x_1 & 2x_3x_2 + 2x_0x_1 & x_0^2 + x_3^2 - x_2^2 - x_1^2 \end{bmatrix} \quad (2)$$

where

$$\begin{aligned} t_1 &= 2x_0y_1 - 2y_0x_1 - 2y_2x_3 + 2y_3x_2, \\ t_2 &= 2x_0y_2 - 2y_0x_2 - 2y_3x_1 + 2y_1x_3, \\ t_3 &= 2x_0y_3 - 2y_0x_3 - 2y_1x_2 + 2y_2x_1. \end{aligned} \quad (3)$$

The point $[(x, y, z)^T$ is transformed to $(x', y', z')^T$ according to

$$(1, x', y', z')^T = \mathbf{M} \cdot (1, x, y, z)^T.$$

The entries (x_i, y_i) in the transformation matrix \mathbf{M} have to fulfill the quadratic identity

$$x_0y_0 + x_1y_1 + x_2y_2 + x_3y_3 = 0 \quad (4)$$

and at least one x_i is different from 0. The lower right 3×3 sub-matrix of \mathbf{M} is an element of the special orthogonal group $SO(3)^+$ and the x_i are the Euler parameters. This representation of Euclidean displacements is sometimes called Study representation and the parameters x_i, y_i are called Study parameters. This allows the following multidimensional geometric interpretation: Eq. (4) defines a six dimensional quadric hyper-surface in a seven dimensional projective space P^7 . This quadric S_6^2 is called *Study quadric* and serves as a point model for Euclidean displacements. The quadric S_6^2 is of hyperbolic type and has the following properties:

1. The maximal linear spaces on S_6^2 are three dimensional (generator spaces).
2. Each tangent space cuts S_6^2 in a five dimensional cone.
3. The generator space $x_0 = x_1 = x_2 = x_3 = 0$ is one of the 3-spaces mentioned above but it does not represent regular displacements, because in this space all Euler parameters are zero. Therefore this space has to be cut out of S_6^2 . A quadric with one generator space removed is called sliced.

A detailed treatment of more properties of S_6^2 can be found in [24, Chapter 10]. The mapping

$$\begin{aligned} \kappa: \mathcal{D} &\rightarrow P \in P^7 & (5) \\ \mathbf{M}(x_i, y_i) &\rightarrow (x_0 : x_1 : x_2 : x_3 : y_0 : y_1 : y_2 : y_3)^T \neq \\ &(0 : 0 : 0 : 0 : 0 : 0 : 0 : 0)^T \end{aligned}$$

is called *kinematic mapping* and maps each Euclidean displacement \mathcal{D} to a point P on $S_6^2 \subset P^7$.

Given a displacement \mathcal{D} as in Eq. (1) it is straightforward to compute the Study parameters x_i, y_i . One can use one of the following formulas to compute the Euler parameters x_i directly from the 3×3 proper orthogonal matrix $\mathbf{A} = (a_{ij})_{i,j=1,\dots,3}$:

$$\begin{aligned}
x_0 : x_1 : x_2 : x_3 &= 1 + a_{11} + a_{22} + a_{33} : a_{32} - a_{23} : a_{13} - a_{31} : a_{21} - a_{12} \\
x_0 : x_1 : x_2 : x_3 &= a_{32} - a_{23} : 1 + a_{11} - a_{22} - a_{33} : a_{12} + a_{21} : a_{31} + a_{13} \\
x_0 : x_1 : x_2 : x_3 &= a_{13} - a_{31} : a_{12} + a_{21} : 1 - a_{11} + a_{22} - a_{33} : a_{23} + a_{32} \\
x_0 : x_1 : x_2 : x_3 &= a_{21} - a_{12} : a_{31} + a_{13} : a_{23} + a_{32} : 1 - a_{11} - a_{22} + a_{33}.
\end{aligned} \tag{6}$$

These formulas are already due to Study [25]. If \mathbf{A} is non-symmetric, we can always take the first proportion of Eq.(6). If \mathbf{A} is symmetric, then it describes a rotation about an angle of π and the first formula fails. In this case we can always resort to one of the three remaining proportions. It should be noted, that at least one of the four proportions in Eq.(6) is nonzero. The y_i are given by

$$\begin{aligned}
y_0 &= -\frac{1}{2}(t_3x_3 + t_2x_2 + t_1x_1), \\
y_1 &= -\frac{1}{2}(t_3x_2 - t_2x_3 - t_1x_0), \\
y_2 &= -\frac{1}{2}(-t_3x_1 + t_1x_3 - t_2x_0), \\
y_3 &= -\frac{1}{2}(-t_3x_0 + t_2x_1 - t_1x_2).
\end{aligned} \tag{7}$$

Remark 1. *Planar displacements and spherical displacements are included in the model presented above. The kinematic image of spherical displacements is obtained from Eq.(2) by setting $y_i = 0$:*

$$\mathbf{M} := \begin{bmatrix} 1 & 0 & 0 & 0 \\ 0 & x_0^2 + x_1^2 - x_3^2 - x_2^2 & -2x_0x_3 + 2x_2x_1 & 2x_3x_1 + 2x_0x_2 \\ 0 & 2x_2x_1 + 2x_0x_3 & x_0^2 + x_2^2 - x_1^2 - x_3^2 & -2x_0x_1 + 2x_3x_2 \\ 0 & -2x_0x_2 + 2x_3x_1 & 2x_3x_2 + 2x_0x_1 & x_0^2 + x_3^2 - x_2^2 - x_1^2 \end{bmatrix}$$

It should be noted, that spherical displacements generate linear 3-spaces on S_6^2 . Because we have ∞^3 points in the Euclidean three space, which can serve as centers for spherical

displacements, there are ∞^3 3-spaces of this type on the Study quadric. The kinematic image of planar displacements could be obtained by setting $y_0 = y_1 = x_2 = x_3 = 0$. The kinematic images of planar displacements also generate 3-spaces on S_6^2 . Because there are ∞^3 planes in the Euclidean three space we have ∞^3 3-spaces on of this type on S_6^2 .

Hyper-planes in P^7 are determined by linear equations in the point coordinates:

$$\mathbf{u}^T \cdot \mathbf{x} = 0 \quad (8)$$

where \mathbf{u} is a 8-tuple. The entries of \mathbf{u} are called hyperplane coordinates and \mathbf{x} describes an arbitrary point X in P^7 . The relation 8 determines the duality in P^7 . The intersection of the hyper-plane with S_6^2 yields a five parametric set of displacements.

For the following it will be important to have an understanding of the effect of coordinate transformations in the Cartesian space to the representation of displacements in the kinematic image space. Let \mathbf{A} be a displacement having the image space coordinates $A(a_0 : a_1 : a_2 : a_3 : a_4 : a_5 : a_6 : a_7)$

$$\mathbf{A} = \frac{1}{\Delta_1} \begin{pmatrix} a_0^2 + a_1^2 + a_2^2 + a_3^2 & 0 & 0 & 0 \\ 2(a_4a_1 - a_5a_0 - a_7a_2 + a_6a_3) & a_0^2 + a_1^2 - a_2^2 - a_3^2 & 2(a_1a_2 - a_0a_3) & 2(a_1a_3 + a_0a_2) \\ 2(a_4a_2 - a_6a_0 - a_5a_3 + a_7a_1) & 2(a_1a_2 + a_0a_3) & a_0^2 - a_1^2 + a_2^2 - a_3^2 & 2(a_2a_3 - a_0a_1) \\ 2(a_4a_3 - a_7a_0 - a_6a_1 + a_5a_2) & 2(a_1a_3 - a_0a_2) & 2(a_2a_3 + a_0a_1) & a_0^2 - a_1^2 - a_2^2 + a_3^2 \end{pmatrix},$$

where $\Delta_1 = a_0^2 + a_1^2 + a_2^2 + a_3^2$. Let furthermore \mathbf{T} be a fixed transformation with image space coordinates $T(t_0 : t_1 : t_2 : t_3 : t_4 : t_5 : t_6 : t_7)$. A change of coordinates in the base system is represented by a left multiplication of the transformation matrix \mathbf{A} with the

coordinate transformation matrix \mathbf{T} . The Study parameters of this matrix product are:

$$\mathbf{t} \circ \mathbf{a} = \Delta \begin{pmatrix} a_0 t_0 - a_1 t_1 - a_2 t_2 - a_3 t_3 \\ a_0 t_1 + a_1 t_0 + t_2 a_3 - t_3 a_2 \\ a_0 t_2 + a_2 t_0 + a_1 t_3 - a_3 t_1 \\ a_0 t_3 + a_3 t_0 + a_2 t_1 - a_1 t_2 \\ a_0 t_4 - a_1 t_5 - a_2 t_6 - a_3 t_7 + a_4 t_0 - a_5 t_1 - a_6 t_2 - a_7 t_3 \\ a_0 t_5 + a_1 t_4 - a_2 t_7 + a_3 t_6 + a_4 t_1 + a_5 t_0 - a_6 t_3 + a_7 t_2 \\ a_0 t_6 + a_1 t_7 + a_2 t_4 - a_3 t_5 + a_4 t_2 + a_5 t_3 + a_6 t_0 - a_7 t_1 \\ a_0 t_7 - a_1 t_6 + a_2 t_5 + a_3 t_4 + a_4 t_3 - a_5 t_2 + a_6 t_1 + a_7 t_0 \end{pmatrix} \quad (9)$$

where

$$\Delta = \frac{a_0 t_0 - a_1 t_1 - a_2 t_2 - a_3 t_3}{(a_0^2 + a_1^2 + a_2^2 + a_3^2)(t_0^2 + t_1^2 + t_2^2 + t_3^2)}.$$

As the Study parameters are homogeneous Δ can be omitted. It is possible to write Eq. (9) as a transformation matrix \mathbf{T}_b in P^7 multiplied by the vector \mathbf{a} :

$$\mathbf{t} \circ \mathbf{a} = \mathbf{T}_b \mathbf{a}$$

where

$$\mathbf{T}_b = \begin{pmatrix} t_0 & -t_1 & -t_2 & -t_3 & 0 & 0 & 0 & 0 \\ t_1 & t_0 & -t_3 & t_2 & 0 & 0 & 0 & 0 \\ t_2 & t_3 & t_0 & -t_1 & 0 & 0 & 0 & 0 \\ t_3 & -t_2 & t_1 & t_0 & 0 & 0 & 0 & 0 \\ t_4 & -t_5 & -t_6 & -t_7 & t_0 & -t_1 & -t_2 & -t_3 \\ t_5 & t_4 & -t_7 & t_6 & t_1 & t_0 & -t_3 & t_2 \\ t_6 & t_7 & t_4 & -t_5 & t_2 & t_3 & t_0 & -t_1 \\ t_7 & -t_6 & t_5 & t_4 & t_3 & -t_2 & t_1 & t_0 \end{pmatrix}. \quad (10)$$

A coordinate transformation in the moving frame is described by right multiplication $\mathbf{A} \cdot \mathbf{T}$. Performing the same procedure as before one obtains the representation of this transformation in the kinematic image space as

$$\mathbf{a} \circ \mathbf{t} = \mathbf{T}_m \mathbf{a}$$

where

$$\mathbf{T}_m = \begin{pmatrix} t_0 & -t_1 & -t_2 & -t_3 & 0 & 0 & 0 & 0 \\ t_1 & t_0 & t_3 & -t_2 & 0 & 0 & 0 & 0 \\ t_2 & -t_3 & t_0 & t_1 & 0 & 0 & 0 & 0 \\ t_3 & t_2 & -t_1 & t_0 & 0 & 0 & 0 & 0 \\ t_4 & -t_5 & -t_6 & -t_7 & t_0 & -t_1 & -t_2 & -t_3 \\ t_5 & t_4 & t_7 & -t_6 & t_1 & t_0 & t_3 & -t_2 \\ t_6 & -t_7 & t_4 & t_5 & t_2 & -t_3 & t_0 & t_1 \\ t_7 & t_6 & -t_5 & t_4 & t_3 & t_2 & -t_1 & t_0 \end{pmatrix}. \quad (11)$$

The index m indicates the transformation in the moving frame. Summarizing the observations above yields

Theorem 1. *Coordinate transformations in the base or moving frame of a manipulator can be written as projective transformations in the kinematic image space. The elements of the matrices describing these transformations are linear in only one of its Study parameters.*

1.1.1 Properties of \mathbf{T}_b and \mathbf{T}_m

Lemma 1. *The matrix product of \mathbf{T}_b and \mathbf{T}_m is commutative.*

Proof. We rewrite the matrices \mathbf{T}_b and \mathbf{T}_m , using the 4×4 matrices \mathbf{A} , \mathbf{B} , \mathbf{C} and \mathbf{D} :

$$\mathbf{T}_b = \begin{pmatrix} \mathbf{A} & \mathbf{0} \\ \mathbf{B} & \mathbf{A} \end{pmatrix} \quad \mathbf{T}_m = \begin{pmatrix} \mathbf{C} & \mathbf{0} \\ \mathbf{D} & \mathbf{C} \end{pmatrix}$$

Then the products are:

$$\mathbf{T}_b \cdot \mathbf{T}_m = \begin{pmatrix} \mathbf{AC} & \mathbf{0} \\ \mathbf{BC} + \mathbf{AD} & \mathbf{AC} \end{pmatrix} \quad \mathbf{T}_m \cdot \mathbf{T}_b = \begin{pmatrix} \mathbf{CA} & \mathbf{0} \\ \mathbf{DA} + \mathbf{CB} & \mathbf{CA} \end{pmatrix}$$

The 4×4 sub matrices \mathbf{A} , \mathbf{B} , \mathbf{C} and \mathbf{D} are well known in geometry. They describe the CLIFFORD-translations in an elliptic space (see Giering [10]). The commutativity of CLIFFORD-translations yields the commutativity of the product of \mathbf{T}_b and \mathbf{T}_m . The same result can be obtained by direct computations. \square

In other words, Lemma 1 expresses that it does not matter which coordinate transformation is performed first in the kinematic image space. This is what one would expect because of the same fact in the Euclidean space.

Lemma 2. *The inverse matrices \mathbf{T}_b^{-1} and \mathbf{T}_m^{-1} can be obtained by the substitution $T \rightarrow \widetilde{T}$, ($t_0 \rightarrow t_0, t_1 \rightarrow -t_1, t_2 \rightarrow -t_2, t_3 \rightarrow -t_3, t_4 \rightarrow t_4, t_5 \rightarrow -t_5, t_6 \rightarrow -t_6, t_7 \rightarrow -t_7$) in \mathbf{T}_b resp. \mathbf{T}_m .*

Proof. Direct computation of $\mathbf{T}_b \cdot \widetilde{\mathbf{T}}_b$ (resp. $\mathbf{T}_m \cdot \widetilde{\mathbf{T}}_m$) yields a multiple of the unit matrix. Because of the homogeneity of the Study-parameters this multiple can be omitted. \square

Lemma 3. *The matrices \mathbf{T}_b and \mathbf{T}_m describe transformations in the kinematic image space, that map points of S_6^2 onto points of S_6^2 . Furthermore, the exceptional generator of this quadric, defined by $x_0 = x_1 = x_2 = x_3 = 0$, is mapped onto itself and points of the quadric in this exceptional 3-space having the equation $y_0^2 + y_1^2 + y_2^2 + y_3^2 = 0$ are mapped onto points on the same quadric.*

Proof. Because of the construction of the matrices \mathbf{T}_b and \mathbf{T}_m the transformed points $\mathbf{T}_b \cdot \mathbf{a}$ and $\mathbf{T}_m \cdot \mathbf{a}$ have to fulfill the equation of S_6^2 . The second part of the lemma is also easy to see. Points in the exceptional generator have coordinates $(0 : 0 : 0 : 0 : y_0 : y_1 : y_2 : y_3)$. Because of the upper right 4×4 zero matrix in \mathbf{T}_b and \mathbf{T}_m , the transformed point

has to lie within this generator and has coordinates $(0 : 0 : 0 : 0 : \bar{y}_0 : \bar{y}_1 : \bar{y}_2 : \bar{y}_3)$. Substitution of these coordinates into the equation $y_0^2 + y_1^2 + y_2^2 + y_3^2 = 0$ yields $(y_1^2 + y_2^2 + y_3^2 + y_4^2)(t_0^2 + t_1^2 + t_2^2 + t_3^2) = 0$. Therefore, if the point lies on this quadric before the transformation, then it is contained in the quadric after the transformation. \square

The transformations \mathbf{T}_b and \mathbf{T}_m are point transformations. In the following the action of coordinate transformations in the Cartesian space on hyper-planes in the kinematic image space is derived.

Lemma 4. *Let \mathbf{T} be a point transformation in P^7 and a point $X \in P^7$ described by \mathbf{x} and*

$$X \rightarrow \tilde{X} = \mathbf{T} \cdot \mathbf{x}.$$

This point transformation transforms the hyperplane with the equation

$$\mathbf{u}^T \cdot \mathbf{x} = 0$$

into the hyperplane

$$\tilde{\mathbf{u}}^T \cdot \tilde{\mathbf{x}} = 0$$

where $\tilde{\mathbf{u}} = (\mathbf{T}^T)^{-1} \cdot \mathbf{u}$. That means that this $(\mathbf{T}^T)^{-1}$ is the corresponding transformation for the hyperplane coordinates \mathbf{u} . Furthermore \mathbf{T} transforms a quadric described by the equation

$$\mathbf{x}^T \cdot \mathbf{A} \cdot \mathbf{x} = 0$$

into the quadric

$$\tilde{\mathbf{x}}^T \cdot \tilde{\mathbf{A}} \cdot \tilde{\mathbf{x}} = 0,$$

where $\tilde{\mathbf{A}} = (\mathbf{T}^T)^{-1} \cdot \mathbf{A} \cdot \mathbf{T}^{-1}$.

Proof. If $\mathbf{u}^T \cdot \mathbf{x} = 0$ and $X \rightarrow \tilde{X} = \mathbf{T} \cdot \mathbf{x}$, then one has to look for a $\tilde{\mathbf{u}}$ such, that $\tilde{\mathbf{u}}^T \cdot \tilde{\mathbf{x}} = \tilde{\mathbf{u}}^T \cdot \mathbf{T} \cdot \mathbf{x} = 0$. This implies that $\mathbf{u}^T = \tilde{\mathbf{u}}^T \cdot \mathbf{T}$ or $\tilde{\mathbf{u}} = (\mathbf{T}^T)^{-1} \mathbf{u}$.

If $\mathbf{x}^T \cdot \mathbf{A} \cdot \mathbf{x} = 0$ and $X \rightarrow \tilde{X} = \mathbf{T} \cdot \mathbf{x}$, then one has to look for a $\tilde{\mathbf{A}}$ such, that $\tilde{\mathbf{x}}^T \cdot \tilde{\mathbf{A}} \cdot \tilde{\mathbf{x}} = (\mathbf{T} \cdot \mathbf{x})^T \cdot \tilde{\mathbf{A}} \cdot \mathbf{T} \cdot \mathbf{x} = \mathbf{x}^T \cdot \mathbf{T}^T \cdot \tilde{\mathbf{A}} \cdot \mathbf{T} \cdot \mathbf{x}$. This implies that $\mathbf{A} = \mathbf{T}^T \cdot \tilde{\mathbf{A}} \cdot \mathbf{T}$ or $\tilde{\mathbf{A}} = (\mathbf{T}^T)^{-1} \cdot \tilde{\mathbf{A}} \cdot \mathbf{T}^{-1}$ \square

1.2 Constraint Varieties for Mechanism Analysis and Synthesis

The basic idea to analyze mechanisms with kinematic mapping is the following: every mechanism generates a certain set of points, curves, surfaces or higher dimensional object of up to five dimensions in the image space. Generally the dimension of the object corresponds to the degree of freedom of the mechanism. If for example one point of the moving system of a spatial mechanical device is bound to move on a surface, the system still has five degrees of freedom. Therefore the mechanical constraint is mapped to a hyper-surface in kinematic image space. From this statement we can conclude that every mechanical system in general can be described by a system of equations. If the constraints are of algebraic nature then the equations are algebraic (polynomials). Revolute joints for example are algebraic constraints. The condition that one point of the moving system is bound to move on a circle or on a sphere are algebraic constraints. For the following we restrict the constraints to algebraic ones.

From algebraic point of view we have then a system of polynomial equations $I = (g_1, \dots, g_n)$, which corresponds to an algebraic variety $V = V(g_1, \dots, g_n)$. The algebraic varieties are the constraint surfaces. With this interpretation it is possible to use all the progress which was made in recent years in solving systems of polynomial equations (see [9]).

We show this idea with a simple example: consider a planar parallel manipulator consisting of a base and a platform linked by three *RPR*-legs (Fig.1). In the so called direct kinematics we are given the design of the manipulator, i.e. the design of base and platform (the coordinates $(B_1, C_1, C_2, a_1, a_2, b_1, b_2, c_1, c_2)$ and the lengths of the legs r_1, r_2, r_3). The task is to find all assembly modes.

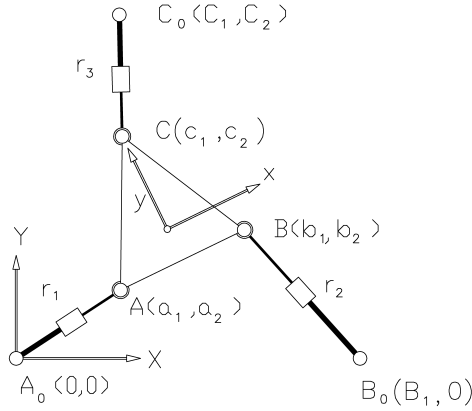


Figure 1: *3RPR*-platform

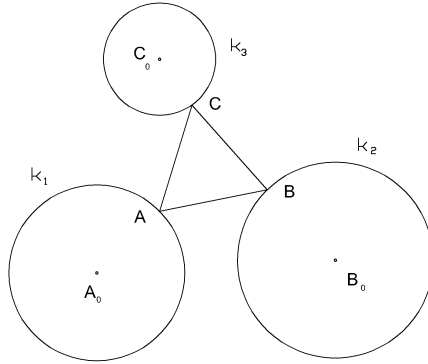


Figure 2: Geometric equivalent

Geometric preprocessing transforms the direct kinematic problem now into the following task: given a triangle and three circles; place the triangle such that its three vertices are on the circles (vertex A on circle k_1 etc., Fig.2). The circles constitute now the mechanical constraints. If for a moment we just consider one circle, then we can say for example that mechanically point A is constrained to move on circle k_1 . Using planar kinematic mapping this constraint is mapped to a hyper-surface in the three dimensional kinematic image space. It turns out that the constraint surface is a special hyperboloid in this space (Fig.3), Bottema-Roth [6]. Algebraically this hyper-surface for the point C is given by the equation:

$$h_1 : \left(y_2 - \frac{1}{2}(c_2 + C_2 - x_1(+C_1 - c_1))\right)^2 + \left(y_3 - \frac{1}{2}(x_1(c_2 - C_2) - C_1 - c_1)\right)^2 - \frac{1}{4}r_3^2(x_1^2 + 1) = 0. \quad (12)$$

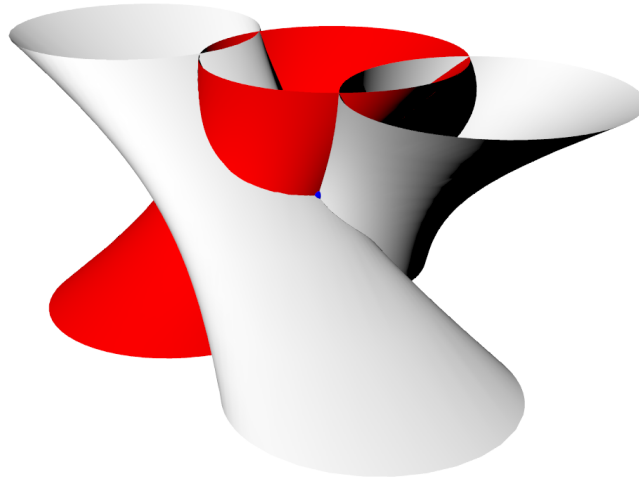


Figure 3: Constraint surfaces in kinematic image space

From algebraic point of view we have three quadratic polynomials h_1, h_2, h_3 which determine the algebraic variety $V = V(h_1, h_2, h_3)$. The dimension of this variety is zero, it consists of 8 points. Six of these points are solutions to the direct kinematics problem, two of the points are always complex and do not solve the task.

2 Application to Mechanism Analysis

In this section we show how the above developed theory is applied to mechanism analysis. We show how the representation of coordinate transformations in the image space helps to simplify the inverse kinematic algorithm presented in Husty et. al.[16, 17]. Furthermore we show how the jump of the dimension of the algebraic solution varieties determine over-constrained $6R$ chains.

It should be noted that this approach was already successfully applied to the analysis of parallel mechanisms to derive the direct kinematics and to determine architecturally singular and pathologically movable platform mechanisms [12, 14, 15].

2.1 Kinematic Image of a 3R Serial Chain

To solve the inverse kinematics of a general $6R$ we will split the $6R$ into two $3R$ chains. Therefore it will be important to derive the kinematic image of $3R$ chains. The advantage of the algorithm developed before is, that we only have to derive the corresponding variety in a canonical form. This means we can place the $3R$ chain in the Cartesian space in the most suitable way and perform the coordinate transformation to a general position in the kinematic image space. This procedure simplifies the necessary computations such that it is possible to write the equations of the constraint manifolds completely general, i.e. without specifying the design parameters.

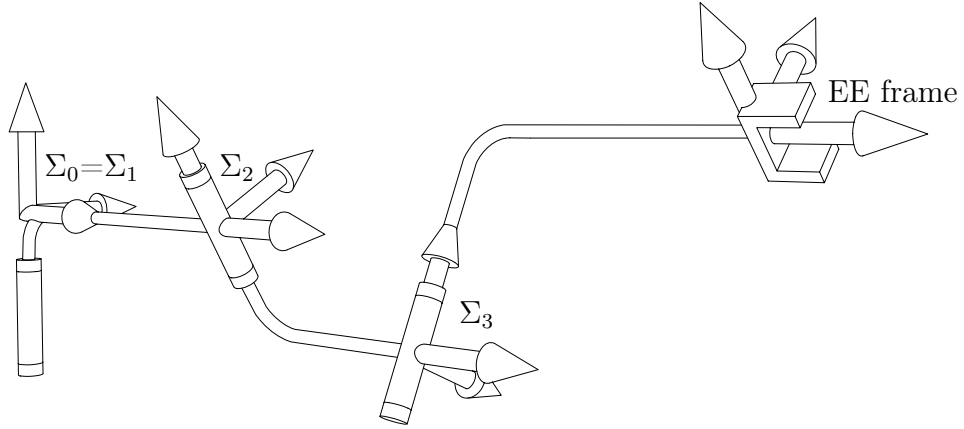


Figure 4: Canonical 3R-manipulator

If the relative position of two rotation axes is described by the usual Denavit-Hartenberg parameters (α_i, a_i, d_i) then the coordinate transformation between the coordinate systems attached to the rotation axes is given by:

$$\mathbf{G} = \begin{pmatrix} 1 & 0 & 0 & 0 \\ a_i & 1 & 0 & 0 \\ 0 & 0 & \cos(\alpha_i) & -\sin(\alpha_i) \\ d_i & 0 & \sin(\alpha_i) & \cos(\alpha_i) \end{pmatrix}. \quad (13)$$

Using this transformation we assume the axes of an nR -chain being in a canonical start

position, where all the axes are parallel to a plane, the first rotation axis is the z-axis of the base coordinate system and the x-axis is the common normal of first and second rotation axis. A simple consideration shows that this is always possible and no restriction of generality (Pfurner [22]). As shown in Fig.4 the rotation axes are always the z-axes of the coordinate systems, therefore we can write these rotations as

$$\mathbf{M}_i = \begin{pmatrix} 1 & 0 & 0 & 0 \\ 0 & \cos(u_i) & -\sin(u_i) & 0 \\ 0 & \sin(u_i) & \cos(u_i) & 0 \\ 0 & 0 & 0 & 1 \end{pmatrix}, \quad (14)$$

u_i being the rotation parameters. The forward kinematics of a general $3R$ chain can be written:

$$\mathbf{D} = \mathbf{B} \cdot \mathbf{M}_1 \cdot \mathbf{G}_1 \cdot \mathbf{M}_2 \cdot \mathbf{G}_2 \cdots \mathbf{M}_3 \cdot \mathbf{G}_3.$$

The constant matrix \mathbf{B} performs the transformation of an arbitrary coordinate system into the canonical base system of Fig.4.

In a step by step procedure the representation of the $3R$ in the image space will be derived. At first we will derive the representation for the canonical chain for which \mathbf{B} is the identity. The transformation that brings the chain into a general position will be performed later in the image space.

If one of the three rotation parameters of the $3R$ -chain is fixed for a moment, then a $2R$ chain remains. The kinematic image of this $2R$ chain is derived first. We have three possibilities to fix a rotation parameter. The procedure is slightly different for each of the three possibilities. We demonstrate the computation for the parameter u_1 . The other two possibilities can be found in Pfurner [22].

Fixing the first revolute axis $u_1 = u_{10}$ (the zero in the index indicates a fixed value)

the corresponding 2R-chain has the matrix representation

$$\mathbf{D} = \mathbf{F} \cdot \mathbf{M}_2 \cdot \mathbf{G}_2 \cdot \mathbf{M}_3 \cdot \mathbf{G}_3.$$

where \mathbf{F} is a fixed transformation, given by $\mathbf{M}_1(u_{10}) \cdot \mathbf{G}_1$. \mathbf{F} and \mathbf{G}_3 are coordinate transformations in the base respectively moving frame of this 2R-chain. Neglecting \mathbf{F} and setting $d_2 = 0$ transforms the chain into a canonical one as shown in Figure 5. Setting $d_2 = 0$ means no loss of generality because a transformation in the direction of the second revolute axis can be achieved later directly in the kinematic image space. Omitting \mathbf{G}_3 transforms the end-effector frame such, that the z -axis coincides with the second axis of this 2R-chain and the x -axis is aligned with the common normal of the two revolute axes.

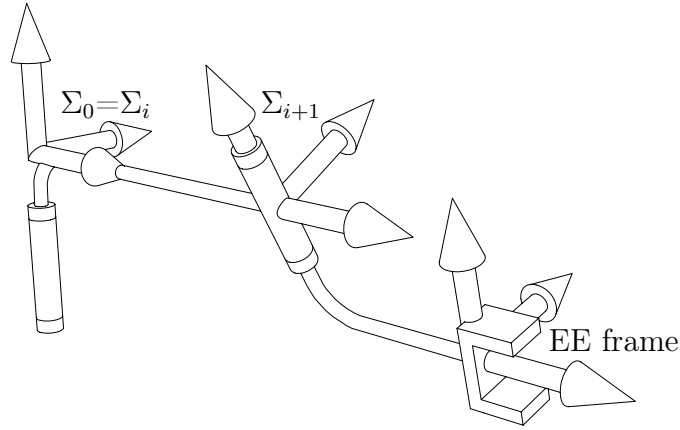


Figure 5: Canonical 2R-mechanism

Then the matrix representation of the remaining 2R-chain becomes

$$\mathbf{D} = \mathbf{M}_2 \cdot \mathbf{G}_2 \cdot \mathbf{M}_3. \quad (15)$$

The parametric representation of the constraint manifold, computed with Eqs. (6) and

(7) reads

$$\begin{pmatrix} x_0 \\ x_1 \\ x_2 \\ x_3 \\ y_0 \\ y_1 \\ y_2 \\ y_3 \end{pmatrix} = \begin{pmatrix} (\cos(u_2) \cos(u_3) - \sin(u_2) \sin(u_3) + 1)(1 + \cos(\alpha_2)) \\ (\cos(u_2) + \cos(u_3)) \sin(\alpha_2) \\ (\sin(u_2) - \sin(u_3)) \sin(\alpha_2) \\ (\cos(u_2) \sin(u_3) + \sin(u_2) \cos(u_3))(1 + \cos(\alpha_2)) \\ \frac{1}{2}a_2(\cos(u_2) \cos(u_3) - \sin(u_2) \sin(u_3) + 1)(\sin \alpha_2) \\ -\frac{1}{2}a_2(\cos(u_2) + \cos(u_3))(1 + \cos(\alpha_2)) \\ -\frac{1}{2}a_2(\sin(u_2) - \sin(u_3))(1 + \cos(\alpha_2)) \\ \frac{1}{2}a_2(\cos(u_2) \sin(u_3) + \sin(u_2) \cos(u_3))(\sin(\alpha_2)) \end{pmatrix}.$$

By inspection and direct substitution one can verify easily that these coordinates satisfy four independent linear equations:

$$\begin{aligned} \overline{Hc}_{11} : a_2 \sin(\alpha_2)x_0 - 2(1 + \cos(\alpha_2))y_0 &= 0 \\ \overline{Hc}_{12} : a_2(1 + \cos(\alpha_2))x_1 + 2 \sin(\alpha_2)y_1 &= 0 \\ \overline{Hc}_{13} : a_2(1 + \cos(\alpha_2))x_2 + 2 \sin(\alpha_2)y_2 &= 0 \\ \overline{Hc}_{14} : a_2 \sin(\alpha_2)x_3 - 2(1 + \cos(\alpha_2))y_3 &= 0 \end{aligned}$$

Applying half tangent substitution ($al_2 = \tan \frac{\alpha_2}{2}$) these equations rewrite to

$$\begin{aligned} \overline{Hc}_{11} : a_2al_2x_0 - 2y_0 &= 0 \\ \overline{Hc}_{12} : a_2x_1 + 2al_2y_1 &= 0 \\ \overline{Hc}_{13} : a_2x_2 + 2al_2y_2 &= 0 \\ \overline{Hc}_{14} : a_2al_2x_3 - 2y_3 &= 0. \end{aligned} \tag{16}$$

Similar equations have been derived by Selig [24].

In the next step we add the rotation about the first axis having the parameter u_1 and a constant transformation in the moving frame to transform it into a general position. In this case one has to apply the (now one parametric set of) coordinate transformations

$\mathbf{M}_1 \cdot \mathbf{G}_1 \cdot \overline{\mathbf{G}}_2$ in the base frame and \mathbf{G}_3 in the moving frame of the $2R$ -chain. $\overline{\mathbf{G}}_2$ translates the base frame by d_2 in the direction of the z -axis (same matrix as \mathbf{G}_2 but $a_2 = 0, \alpha_2 = 0$). This is the new and essential contribution of this work that the transformations bringing the canonical manifolds to a general position can be performed efficiently in the kinematic image space. Although the theory seems to be a bit complicated, its application makes the necessary computation simple.

The necessary transformations are executed directly on the hyper-planes of Eq. (16) which describe the canonical $2R$ -chain in the kinematic image space. The point transformation in the base frame would be $\mathbf{T}_b(\mathbf{M}_1) \cdot \mathbf{T}_b(\mathbf{G}_1) \cdot \mathbf{T}_b(\overline{\mathbf{G}}_2)$, so according to Lemma 4 the hyperplane transformation is $((\mathbf{T}_b(\mathbf{M}_1) \cdot \mathbf{T}_b(\mathbf{G}_1) \cdot \mathbf{T}_b(\overline{\mathbf{G}}_2))^T)^{-1} = (\mathbf{T}_b(\mathbf{M}_1)^T)^{-1} \cdot (\mathbf{T}_b(\mathbf{G}_1)^T)^{-1} \cdot (\mathbf{T}_b(\overline{\mathbf{G}}_2)^T)^{-1}$. After applying the half tangent substitutions for all angles ($v_1 = \tan \frac{u_1}{2}, a_{l_i} = \tan \frac{\alpha_i}{2}, i = 1, 2$) these transformations write

$$(\mathbf{T}_b(\mathbf{M}_1)^T)^{-1} = \begin{pmatrix} 1 & 0 & 0 & -v_1 & 0 & 0 & 0 & 0 \\ 0 & 1 & -v_1 & 0 & 0 & 0 & 0 & 0 \\ 0 & v_1 & 1 & 0 & 0 & 0 & 0 & 0 \\ v_1 & 0 & 0 & 1 & 0 & 0 & 0 & 0 \\ 0 & 0 & 0 & 0 & 1 & 0 & 0 & -v_1 \\ 0 & 0 & 0 & 0 & 0 & 1 & -v_1 & 0 \\ 0 & 0 & 0 & 0 & 0 & v_1 & 1 & 0 \\ 0 & 0 & 0 & 0 & v_1 & 0 & 0 & 1 \end{pmatrix},$$

$$(\mathbf{T}_b(\mathbf{G}_1)^T)^{-1} = \begin{pmatrix} 2 & -2al_1 & 0 & 0 & al_1a_1 & a_1 & al_1 & 0 \\ 2al_1 & 2 & 0 & 0 & -a_1 & al_1a_1 & 0 & -al_1 \\ 0 & 0 & 2 & -2al_1 & -al_1 & 0 & al_1a_1 & a_1 \\ 0 & 0 & 2al_1 & 2 & 0 & al_1 & -a_1 & al_1a_1 \\ 0 & 0 & 0 & 0 & 2 & -2al_1 & 0 & 0 \\ 0 & 0 & 0 & 0 & 2al_1 & 2 & 0 & 0 \\ 0 & 0 & 0 & 0 & 0 & 0 & 2 & -2al_1 \\ 0 & 0 & 0 & 0 & 0 & 0 & 2al_1 & 2 \end{pmatrix},$$

$$(\mathbf{T}_b(\overline{\mathbf{G}}_2)^T)^{-1} = \begin{pmatrix} 2 & 0 & 0 & 0 & 0 & 0 & 0 & d_2 \\ 0 & 2 & 0 & 0 & 0 & 0 & d_2 & 0 \\ 0 & 0 & 2 & 0 & 0 & -d_2 & 0 & 0 \\ 0 & 0 & 0 & 2 & -d_2 & 0 & 0 & 0 \\ 0 & 0 & 0 & 0 & 2 & 0 & 0 & 0 \\ 0 & 0 & 0 & 0 & 0 & 2 & 0 & 0 \\ 0 & 0 & 0 & 0 & 0 & 0 & 2 & 0 \\ 0 & 0 & 0 & 0 & 0 & 0 & 0 & 2 \end{pmatrix}.$$

The coordinate transformation \mathbf{G}_3 in E^3 of the moving frame can be performed with help of

$$(\mathbf{T}_m(\mathbf{G}_3)^T)^{-1} = \begin{pmatrix} 2 & -2al_3 & 0 & 0 & al_3a_3 & a_3 & al_3d_3 & d_3 \\ 2al_3 & 2 & 0 & 0 & -a_3 & al_3a_3 & -d_3 & al_3d_3 \\ 0 & 0 & 2 & 2al_3 & -al_3d_3 & d_3 & al_3a_3 & -a_3 \\ 0 & 0 & -2al_3 & 2 & -d_3 & -al_3d_3 & a_3 & al_3a_3 \\ 0 & 0 & 0 & 0 & 2 & -2al_3 & 0 & 0 \\ 0 & 0 & 0 & 0 & 2al_3 & 2 & 0 & 0 \\ 0 & 0 & 0 & 0 & 0 & 0 & 2 & 2al_3 \\ 0 & 0 & 0 & 0 & 0 & 0 & -2al_3 & 2 \end{pmatrix},$$

where $al_3 = \alpha_3$, in P^7 . Applying all transformations of the base and moving frames on the hyper-plane coordinates of the hyper-planes in Eq. (16) yields the four linear equations:

$Hc_1(v_1)$:

$$\begin{aligned}
& (a_2al_2 - v_1d_2 - al_3a_1 - al_3a_3 - al_1a_1 - a_2al_2al_3al_1 - al_3v_1d_2al_1 - al_3d_3al_1v_1 - a_3al_1 - d_3v_1)x_0 + \\
& (-al_3v_1d_2 + a_2al_2al_3 + a_2al_2al_1 + a_1 + a_3 - al_3al_1a_1 + v_1d_2al_1 - al_3a_3al_1 + d_3al_1v_1 - al_3d_3v_1)x_1 + \\
& (a_1v_1 - d_2al_1 + al_3d_3 - d_3al_1 + a_2al_2al_1v_1 + al_3d_2 - al_3al_1a_1v_1 - al_3a_3al_1v_1 + a_3v_1 + a_2al_2al_3v_1)x_2 + \\
& (-a_3al_1v_1 + d_2 + d_3 - al_1a_1v_1 + a_2al_2v_1 - al_3a_1v_1 + al_3d_2al_1 + al_3d_3al_1 - a_2al_2al_3al_1v_1 - al_3a_3v_1)x_3 + \\
& 2(al_3al_1 - 1)y_0 - 2(al_3 + al_1)y_1 - 2(al_1v_1 + al_3v_1)y_2 + 2(al_3al_1v_1 - v_1)y_3 = 0
\end{aligned} \tag{17}$$

$Hc_2(v_1)$:

$$\begin{aligned}
& (al_2a_1 + al_2v_1d_2al_1 - a_2al_1 - al_2al_3al_1a_1 - al_2al_3a_3al_1 - al_2al_3v_1d_2 - al_2d_3al_1v_1 - a_2al_3 + al_2a_3 + \\
& al_2al_3d_3v_1)x_0 + (-a_2al_3al_1 + al_2v_1d_2 - al_2al_3d_3al_1v_1 + al_2al_3a_1 + al_2al_3a_3 - al_2d_3v_1 + al_2al_1a_1 + \\
& al_2a_3al_1 + a_2 + al_2al_3v_1d_2al_1)x_1 + (al_2d_3 - al_2d_2 + al_2al_3a_1v_1 - al_2al_3d_2al_1 - a_2al_3al_1v_1 + al_2al_1a_1v_1 + \\
& al_2al_3a_3v_1 + al_2a_3al_1v_1 + al_2al_3d_3al_1 + a_2v_1)x_2 + (al_2a_1v_1 - a_2al_3v_1 - al_2d_2al_1 + al_2al_3d_2 - al_2al_3d_3 + \\
& al_2a_3v_1 + al_2d_3al_1 - al_2al_3al_1a_1v_1 - al_2al_3a_3al_1v_1 - a_2al_1v_1)x_3 - 2(al_2al_3 + al_2al_1)y_0 + 2(-al_2al_3al_1 + \\
& al_2)y_1 + 2(al_2v_1 - al_2al_3al_1v_1)y_2 - 2(al_2al_3v_1 + al_2al_1v_1)y_3 = 0
\end{aligned} \tag{18}$$

$Hc_3(v_1)$:

$$\begin{aligned}
& (-al_2a_3v_1 + al_2al_3d_3 + al_2a_1v_1 - al_2d_2al_1 - al_2al_3d_2 + al_2al_3al_1a_1v_1 - al_2al_3a_3al_1v_1 + al_2d_3al_1 - \\
& a_2al_1v_1 + a_2al_3v_1)x_0 + (-al_2al_3a_3v_1 + al_2al_3d_3al_1 - a_2v_1 + al_2d_2 - al_2d_3 - a_2al_3al_1v_1 + al_2al_3a_1v_1 - \\
& al_2al_3d_2al_1 - al_2al_1a_1v_1 + al_2a_3al_1v_1)x_1 + (a_2al_3al_1 + a_2 - al_2al_3v_1d_2al_1 + al_2v_1d_2 + al_2al_1a_1 + \\
& al_2al_3d_3al_1v_1 - al_2d_3v_1 + al_2al_3a_3 - al_2a_3al_1 - al_2al_3a_1)x_2 + (a_2al_1 - al_2a_1 + al_2a_3 - al_2al_3v_1d_2 - \\
& al_2al_3al_1a_1 - al_2v_1d_2al_1 + al_2d_3al_1v_1 + al_2al_3d_3v_1 - a_2al_3 + al_2al_3a_3al_1)x_3 + 2(al_2al_3v_1 - \\
& al_2al_1v_1)y_0 - 2(al_2v_1 + al_2al_3al_1v_1)y_1 + 2(al_2al_3al_1 + al_2)y_2 + 2(-al_2al_3 + al_2al_1)y_3 = 0
\end{aligned} \tag{19}$$

$Hc_4(v_1) :$

$$\begin{aligned}
& (-d_2 + al_3a_3v_1 - d_3 - a_3al_1v_1 + al_3d_3al_1 - a_2al_2al_3al_1v_1 - a_2al_2v_1 + al_1a_1v_1 - al_3a_1v_1 + al_3d_2al_1)x_0 + \\
& (a_1v_1 - d_2al_1 - al_3d_2 - a_2al_2al_3v_1 + a_2al_2al_1v_1 + al_3al_1a_1v_1 - al_3a_3al_1v_1 - a_3v_1 - d_3al_1 - al_3d_3)x_1 + \\
& (a_2al_2al_3 + al_3a_3al_1 - v_1d_2al_1 - d_3al_1v_1 - a_2al_2al_1 - a_1 + a_3 - al_3v_1d_2 - al_3al_1a_1 - al_3d_3v_1)x_2 + \\
& (a_2al_2 + a_3al_1 - al_3a_3 - al_1a_1 + al_3a_1 - d_3v_1 + a_2al_2al_3al_1 + al_3v_1d_2al_1 + al_3d_3al_1v_1 - v_1d_2)x_3 + \\
& 2(al_3al_1v_1 + v_1)y_0 + 2(al_3v_1 - al_1v_1)y_1 + 2(al_1 - al_3)y_2 + -2(1 + al_3al_1)y_3 = 0
\end{aligned} \tag{20}$$

Each of the hyper-planes Hc_i depends on the parameter v_1 . Intersecting this set of hyperplane equations yields a one parameter set of 3-spaces $T_c(v_1)$ whose intersection with the Study quadric is the constraint manifold of the canonical serial 3R-chain.

Remark 1. *It has to be emphasized that the presented algorithm allows to write the equations completely general, i.e. without specifying the DH parameters.*

Remark 2. *Almost the same procedure can be done with the other two possibilities. One can fix u_2 or u_3 and obtains in each case a one parameter set of 3-spaces $T_c(v_2)$ and $T_c(v_3)$ with v_2 and v_3 being the algebraic values of u_2 and u_3 . It should be noted that the intersection of each of these sets of 3-spaces and S_6^2 yields the same constraint manifold. The two other possibilities just provide a redundant description of the constraint manifold. It is advantageous to have this description to handle all special cases that can occur (see next remark).*

Remark 3. *The intersection of $T_c(v_1)$ and S_6^2 fails if lies on S_6^2 . This happens when the second and the third revolute axes are parallel or intersect. In this cases one has to take another set of hyperplane equations $T_c(v_2)$ or $T_c(v_3)$ to compute the constraint manifold.*

Remark 4. *If the 3R-chain is planar or spherical the equations of the hyper-planes sim-*

plify considerable. In the planar case we have:

$$\begin{aligned}
H_{c_{p1}} : & & -al_3x_0 + x_1 &= 0 \\
H_{c_{p2}} : & & x_2 - al_3x_3 &= 0 \\
H_{c_{p3}} : & al_3a_3x_0 - a_3x_1 - al_3d_3x_2 - d_3x_3 + 2y_0 + 2al_3y_1 &= 0 \\
H_{c_{p4}} : & d_3x_0 + al_3d_3x_1 - a_3x_2 + al_3a_3x_3 + 2al_3y_2 + 2y_3 &= 0.
\end{aligned} \tag{21}$$

and in the spherical case the equations are:

$$\begin{aligned}
H_{c_{w1}} : & al_3a_3x_0 - a_3x_1 - al_3d_3x_2 - d_3x_3 + 2y_0 + 2al_3y_1 = 0 \\
H_{c_{w2}} : & a_3x_0 + al_3a_3x_1 + d_3x_2 - al_3d_3x_3 - 2al_3y_0 + 2y_1 = 0 \\
H_{c_{w3}} : & al_3d_3x_0 - d_3x_1 + al_3a_3x_2 + a_3x_3 + 2y_2 - 2al_3y_3 = 0 \\
H_{c_{w4}} : & d_3x_0 + al_3d_3x_1 - a_3x_2 + al_3a_3x_3 + 2al_3y_2 + 2y_3 = 0.
\end{aligned} \tag{22}$$

The last step is now to introduce the general case. It differs from the canonical $3R$ -chains by having a general position of the first revolute axis with respect to the fixed coordinate system (see Figure 6).

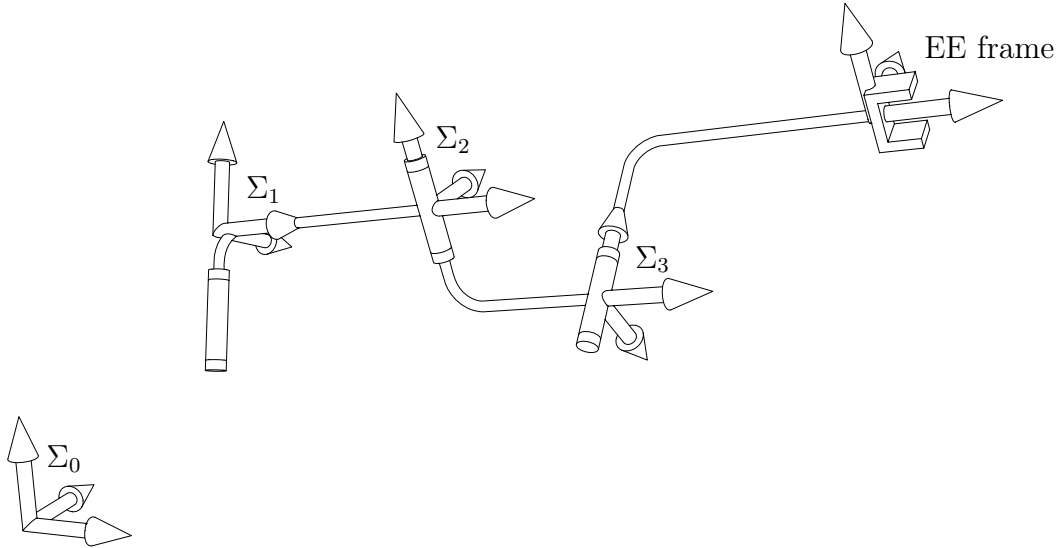


Figure 6: General $3R$ -serial-chain

Up to now the $3R$ -chain was always a canonical one, which means that the first axis is coincident with the z -axis of the base frame and the DH-parameter d_1 is equal to zero. To

derive from the constraint manifold of the canonical 3R-chain the equations of the constraint manifold of an arbitrarily placed 3R-chain only a fixed coordinate transformation in the base frame is needed. This can be executed directly in the kinematic image space via the matrix $(\mathbf{T}_b^T)^{-1}$ (Eq.10). Applied to the one parameter sets of 3-spaces $T_c(v_1), T_c(v_2)$ and $T_c(v_3)$, generated as intersections of the one parameter sets of hyper-planes in Eqs. (17) - (20), resp. the hyperplane equations of $T_c(v_2)$ and $T_c(v_3)$. We also have to apply this transformation to the fixed 3-spaces T_{cp} and T_{cw} , generated as the intersections of the hyper-planes in Eqs. (21) and (22). This procedure yields new sets of hyper-plane equations intersecting in one parameter sets of 3-spaces resp. fixed 3-spaces. The resulting one parameter sets of 3-spaces will be denoted by $T(v_1), T(v_2)$ and $T(v_3)$. The hyperplane equations describing these sets of 3-spaces are a little bit more complicated. Because of limit of space they are not displayed here. They consist of approximately 200 terms and it should be noted that they still can be computed completely general, i.e. without specifying the DH-parameters. A complete listing of the general equations can be found in Pfuner [22].

The hyper-plane equations describing the fixed 3-space as the constraint manifold T_p of an arbitrary planar 3R-mechanism, where the first axis does not coincide with the z -axis of the base frame, are

$$\begin{aligned}
H_{p1} : & -2x_0(t_0al_3 + t_1) + 2x_1(-t_1al_3 + t_0) + 2x_2(-t_2al_3 + t_3) - 2x_3(t_3al_3 + t_2) = 0, \\
H_{p2} : & 2x_0(-t_2 + t_3al_3) - 2x_1(t_3 + t_2al_3) + 2x_2(t_0 + t_1al_3) + 2x_3(t_1 - t_0al_3) = 0, \\
H_{p3} : & x_0(t_0al_3a_3 + t_1a_3 + t_2al_3d_3 + t_3d_3 + 2t_4 - 2t_5al_3) + x_1(t_1al_3a_3 - t_0a_3 + t_3al_3d_3 - t_2d_3 + 2t_5 + \\
& 2t_4al_3) + x_2(t_2al_3a_3 - t_3a_3 - t_0al_3d_3 + t_1d_3 + 2t_6 + 2t_7al_3) + x_3(t_3al_3a_3 + t_2a_3 - t_1al_3d_3 - \\
& t_0d_3 + 2t_7 - 2t_6al_3) + 2y_0(-t_1al_3 + t_0) + 2y_1(t_1 + t_0al_3) + 2y_2(t_2 + t_3al_3) + 2y_3(t_3 - t_2al_3) = 0, \\
H_{p4} : & x_0(t_0d_3 - t_1al_3d_3 + t_2a_3 - t_3al_3a_3 - 2t_6al_3 - 2t_7) + x_1(t_1d_3 + t_0al_3d_3 + t_3a_3 + t_2al_3a_3 - \\
& 2t_7al_3 + 2t_6) + x_2(t_2d_3 + t_3al_3d_3 - t_0a_3 - t_1al_3a_3 + 2t_4al_3 - 2t_5) + x_3(t_3d_3 - t_2al_3d_3 - t_1a_3 + \\
& t_0al_3a_3 + 2t_5al_3 + 2t_4) - 2y_0(t_3 + t_2al_3) + 2y_1(t_2 - t_3al_3) + 2y_2(t_0al_3 - t_1) + 2y_3(t_0 + t_1al_3) = 0.
\end{aligned} \tag{23}$$

The remarkable result of this section is that we have found a completely general description of all possible $3R$ -chains. The equations do not have to be computed once more for different designs. The design parameters can be substituted directly into the four hyperplane equations. Additionally we have a redundant description of the generated one parameter sets of 3-spaces, so one only has to be aware about the layout of the chain to take the appropriate set of equations. This process can be fully automated.

2.2 Properties of the constraint manifolds

To pass from the constraint manifolds of a canonical $3R$ -chain to those of a general, arbitrary $3R$ -chain only a fixed coordinate transformation in the base frame was applied. It is important to observe that this transformation does not change the geometric shape and geometric properties of the manifold, but only the position in the kinematic image space. Therefore the geometric properties for the manifolds $T(v_i)$ can be derived directly from $T_c(v_i)$, $i = 1, 2, 3$. The transformation from canonical form to general position will not change the geometric properties.

The one parameter sets of 3-spaces $T(v_1)$, $T(v_2)$ and $T(v_3)$ are well known in geometry. Geometrically they can be obtained by the following algorithm: Take two 3-spaces in P^7 and define a linear relation between the points in these spaces what means, that each point of one space is joined by a line with exactly one point of the other three space. The manifold of all these lines is called a Segre manifold. A symbolic sketch of a Segre manifold is depicted in Fig. 7. In this figure 3-spaces, corresponding to discrete values of v_1 , are drawn as boxes. Through every point of such a 3-space there is exactly one line that belongs to the manifold. As an example $\mathbf{p}(v_1)$ is drawn. An lower dimensional example of a Segre manifold is a hyperboloid in E^3 . There one has to take two lines instead of the 3-spaces in P^7 and a linear relation between the points on both lines. The lines connecting the corresponding points are a regulus of a hyperboloid, a Segre manifold in P^3 . More general a Segre manifold can be defined as a topological product of two

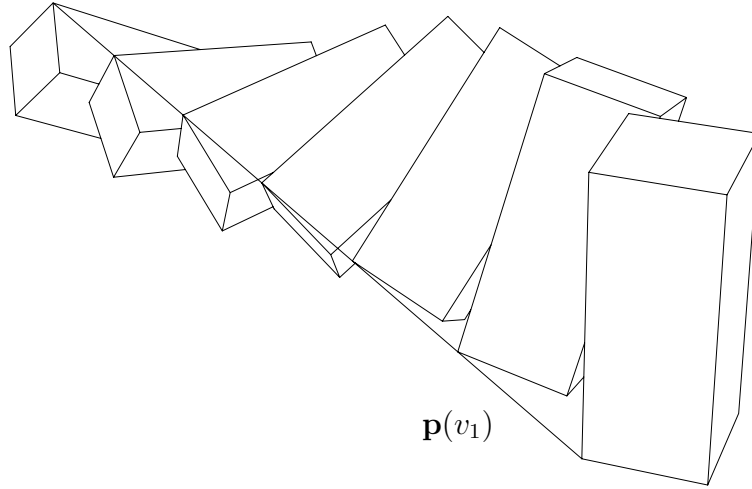


Figure 7: Symbolic sketch of SM_1

linear spaces, i.e., the manifold of all ordered pairs of points of both spaces (see Naas and Schmid [21]).

Definition 1. *The Segre manifolds generated by the one parameter set of 3-spaces $T(v_1)$, $T(v_2)$ resp. $T(v_3)$ are denoted by SM_1, SM_2 resp. SM_3 . The Segre manifolds generated by the one parameter set of 3-spaces $T_c(v_1), T_c(v_2)$ resp. $T_c(v_3)$ are denoted by SM_{1c}, SM_{2c} resp. SM_{3c} .*

Summarizing the findings above one can state:

Theorem 2. *The Segre manifold SM_1 (SM_2, SM_3) is the intersection of four one parameter pencils of hyper-planes. The hyper-plane coordinates depend linearly on v_1 (v_2, v_3).*

Furthermore we can state:

Theorem 3. *The constraint manifold of a 3R-chain is the intersection of the Study-quadric with a Segre manifold SM_1 (SM_2, SM_3) generated by the pencils of hyperplanes describing $T(v_1)$ ($T(v_2), T(v_3)$).*

Corollary 1. *The constraint manifold of a 3R-chain is the intersection of any two of the Segre manifolds SM_1, SM_2, SM_3 .*

2.2.1 Different representations of the Segre manifold

This section describes different representations of the Segre manifolds $SM_i, i = 1, 2, 3$. As stated above all three manifolds have the same intersection with S_6^2 and describe therefore the same set of displacements. Note that the difference between the three manifolds are points outside of S_6^2 . It has turned out that one has to switch between the different descriptions when special layouts like parallelism of rotation axes occur.

Parametric representation, span of points Specify one arbitrary 3-space of $T(v_1)$ by fixing the parameter $v_1 = v_{10}$. Choose four linearly independent points \mathbf{p}_k ($k = 1, \dots, 4$) of this space and then let v_1 vary again. Because of Theorem 2 this results in four straight lines l_k and $\mathbf{p}_k(v_1) = T(v_1) \cap l_k$. Now the points of SM_i are described by

$$\mathbf{x} = \sum_{k=1}^4 \lambda_k \mathbf{p}_k(v_1)$$

where $(\lambda_1, \lambda_2, \lambda_3, \lambda_4)^T$ is a homogeneous quadruple. In this representation, the algebraic degree of SM_i is easily computed. It is defined as the number of intersection points of SM_i and a generic 3-space $U \subset P^7$ (see Harris [11]). Let U be the span of four points described by $\mathbf{u}_1, \dots, \mathbf{u}_4$. U and $T(v_1)$ intersect if and only if

$$\det(\mathbf{p}_1(v_1), \mathbf{p}_2(v_1), \mathbf{p}_3(v_1), \mathbf{p}_4(v_1), \mathbf{u}_1, \mathbf{u}_2, \mathbf{u}_3, \mathbf{u}_4) = 0.$$

This is a polynomial of degree four in v_1 . Hence there exist four intersection points of SM_i and U . That means that the algebraic degree of SM_i is four.

Algebraic equations In order to find a set of algebraic equations of SM_i one has to fix two parameter values v_{11} and v_{12} and let $\mathbf{p}_{jk} = \mathbf{p}_j(v_k)$ for $j = 1, \dots, 4$ and $k = 1, 2$. In a projective coordinate frame with base points $\mathbf{p}_{11}, \dots, \mathbf{p}_{41}, \mathbf{p}_{12}, \dots, \mathbf{p}_{42}$ one may use the coordinate vectors $(\xi_0 : \dots : \xi_3 : \eta_0 : \dots : \eta_3)^T$. In this frame, the algebraic equations

of SM_i read

$$\det \begin{pmatrix} \xi_k & \eta_l \\ \xi_l & \eta_k \end{pmatrix} = 0, \quad k, l, \in 0, \dots, 3 \quad (24)$$

(see Naas et.al. [21]). Note that only three of these quadric equations are independent. Therefore, SM_i is the intersection of three hyper-quadrics. In order to find the equations of SM_i in the original coordinate frame of P^7 , one has to apply the transformation $\mathbf{y} = \mathbf{P}\mathbf{x}$ where \mathbf{P} is the matrix

$$\mathbf{P} = (\mathbf{p}_{11}, \dots, \mathbf{p}_{41}, \mathbf{p}_{12}, \dots, \mathbf{p}_{42})$$

to the coordinates in Eq. (24). There exist symmetric eight by eight matrices such that Eq. (24) reads

$$(\xi_0, \dots, \xi_3, \eta_0, \dots, \eta_3)^T \cdot \mathbf{A}_{ij} \cdot (\xi_0, \dots, \xi_3, \eta_0, \dots, \eta_3) = 0.$$

The transformed equations are (see Lemma 4)

$$(\xi_0, \dots, \xi_3, \eta_0, \dots, \eta_3)^T \cdot (\mathbf{P}^T)^{-1} \mathbf{A}_{ij} \mathbf{P}^{-1} \cdot (\xi_0, \dots, \xi_3, \eta_0, \dots, \eta_3) = 0.$$

Remark 5. *It is possible to compute symbolically the system of algebraic equations of all Segre manifolds without specifying the DH-parameters.*

Intersection of hyperplanes As investigated in Section 2.1 the constraint manifold of an arbitrary $3R$ -chain is the intersection of a one parameter set of 3-spaces, depending linearly on the parameter, with S_6^2 . A fixed 3-space in the seven dimensional projective space is geometrically determined by intersecting four hyper-planes H_1, \dots, H_4 . Algebraically this means it is given by four linear equations. A one parameter set of three spaces is therefore given by the intersection of four one parameter sets of hyper-planes $H_i(v), i = 1, \dots, 4$, each depending linearly on the parameter v . This parameter can be any of the algebraic values of the rotation angles of the $3R$ -chain. Such a linear one pa-

parameter set of hyper-planes is called a pencil of hyper-planes. For each value of v the four pencils of hyper-planes intersect in one three space of the Segre manifold. The advantage of these hyper-plane equations to those presented in Husty et al. [17] is, that because of the newly introduced algorithm these equations are extremely short (224 operands) although no DH-parameter is specified. Additionally all the DH-parameters appear only multilinear within these equations.

Remark 6. *The Segre manifolds have some interesting properties. From kinematic point of view the most interesting is the following: The Segre manifolds SM_1 , SM_2 (with the restriction that $\alpha_1 = 0$ or $\alpha_2 = 0$) and SM_3 intersect the exceptional generator of S_6^2 (the 3-space, that had to be sliced out of the Segre manifold), given by $x_0 = x_1 = x_2 = x_3 = 0$, in conjugate complex lines. These lines lie in those 3-spaces of the Segre manifolds that correspond to the parameter values $v_i = \pm I$, $i = 1, 2, 3$. Furthermore these lines lie on the quadric $y_0^2 + y_1^2 + y_2^2 + y_3^2 = 0$ in this exceptional 3-space.*

This property is important because it shows that the exceptional generator plays in spatial kinematics a similar role as the circle points in planar kinematics. A strict proof of the statement above can be found in Pfunner[22].

2.3 Discussion of the Inverse Kinematics of General 6R-Manipulators

In this subsection we show how the constraint manifolds of $3R$ -chains can be used to solve the inverse kinematics of a general open $6R$ manipulator. Recall that in the inverse kinematic problem of a serial chain the design and a pose of the end-effector of the manipulator is known. The rotation angles u_i of the revolute joints have to be computed.

To apply the theory developed before one has to break up the link between the third and the fourth revolute axis to obtain two $3R$ chains. It has turned out that the best way to do this is the following: We break up at the foot of the common normal of third and fourth axis on the fourth axis. Moreover one has to attach two copies of a coordinate

frame $\Sigma_L = \Sigma_R$, called the "left" and the "right" frame, to the resulting mechanisms in the following way:

- The origin is the foot of the common normal of the third and fourth axis on the fourth axis,
- the x -axis is aligned with the common normal of the third and fourth axes and
- the z -axis coincides with the fourth axis.

The resulting mechanisms are two open $3R$ -chains, called the "left" and the "right" $3R$ -chain. The base frame of the left one is Σ_0 and the EE frame is Σ_L , the base of the right one is Σ_6 with the EE Σ_R (see Fig. 8).

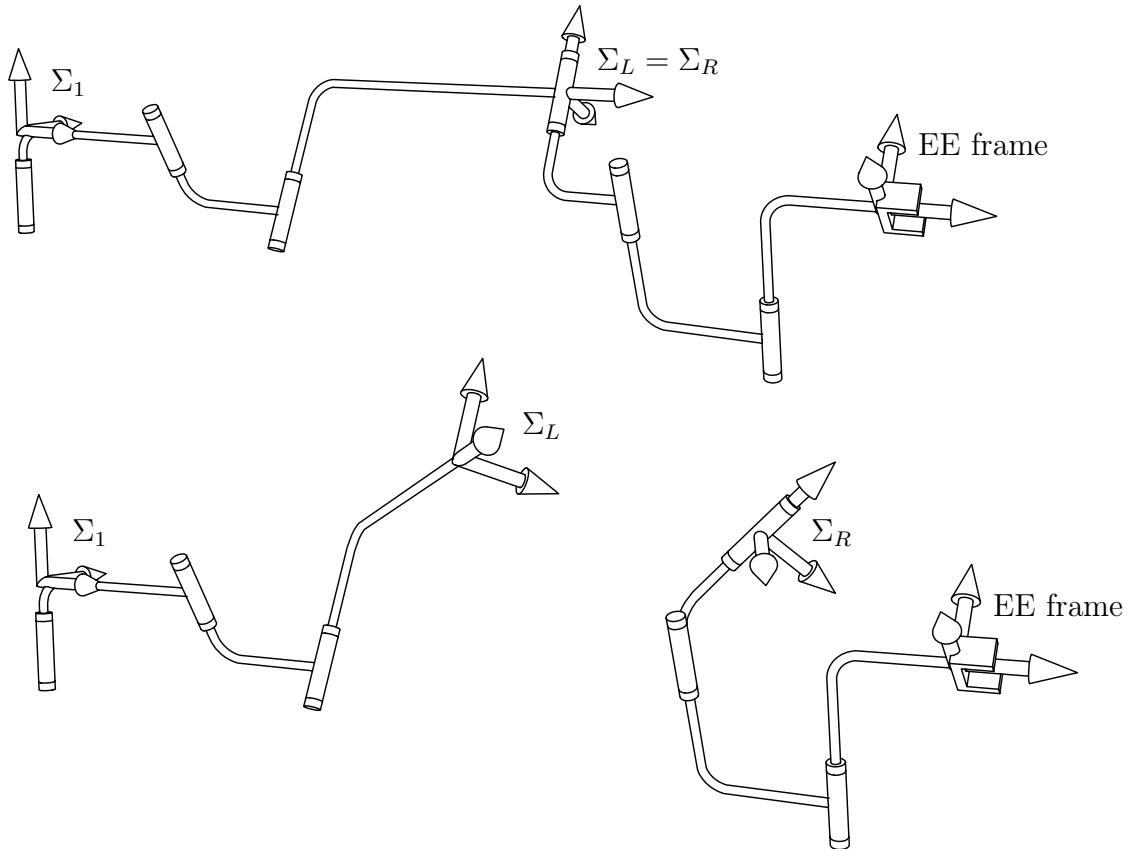


Figure 8: Cutting of the 6R into two 3R serial chains

The pose of Σ_L with respect to Σ_0 is given by

$$\mathbf{T}_1 = \mathbf{M}_1 \cdot \mathbf{G}_1 \cdot \mathbf{M}_2 \cdot \mathbf{G}_2 \cdot \mathbf{M}_3 \cdot \mathbf{G}_3. \quad (25)$$

This is exactly the canonical $3R$ -chain for which the canonical constraint manifold was developed. This manifold was the intersection of one of the Segre manifolds SM_{1c} , SM_{2c} or SM_{3c} resp. the intersection of one of the 3-spaces T_{cp} or T_{cw} with the Study quadric. Which one of the constraint manifolds has to be taken depends on the DH parameters of the 6R-manipulator because in some special cases one or more of the Segre manifolds lie completely on S_6^2 .

The pose of Σ_R with respect to Σ_6 is given by

$$\mathbf{T}_2 = \mathbf{A} \cdot \mathbf{G}_6^{-1} \cdot \mathbf{M}_6^{-1} \cdot \mathbf{G}_5^{-1} \cdot \mathbf{M}_5^{-1} \cdot \mathbf{G}_4^{-1} \cdot \mathbf{M}_4^{-1}. \quad (26)$$

To achieve the representation of the constraint manifold of this right $3R$ -chain one has to take the hyperplane equations representing $T(v_1)$, $T(v_2)$ and $T(v_3)$ for an arbitrary design or the hyperplane equations representing T_p in Eqs. (23) resp. T_w for special designs.

Pfurner [22] has shown that one can adapt the coordinate systems slightly to get the simplest set of equations. After these substitutions the one parameter sets of 3-spaces are denoted by $T(v_6)$, $T(v_5)$ resp. $T(v_4)$, and each of them describes also a Segre manifold denoted by SM_6 , SM_5 resp. SM_4 . Each of them can serve as SM_R . The four pencils of hyper-planes corresponding to each Segre manifold are denoted by $H_5(v_i), \dots, H_8(v_i)$ for $i = 4, 5, 6$. The representations of the fixed 3-spaces are denoted by \bar{T}_p and \bar{T}_w .

The solution of the inverse kinematics problem of a serial 6R-chain can therefore be computed as the intersection

$$S_6^2 \cap SM_L \cap SM_R. \quad (27)$$

With the understanding that a fixed 3-space is a special case of a one parameter set of 3-spaces one may summarize these results in

Theorem 4. *Geometrically the solution of the inverse kinematic problem of a serial 6R-chain is equivalent to the intersection of eight one parameter sets of hyper-planes with S_6^2 in P^7 .*

An investigation of the structure of the nine equations addressed in Theorem 4 reveals the non-linearity of the problem. There are eight hyperplane equations H_i which are linear in x_i, y_i and bilinear in $x_i v_q$ and $y_i v_q$ respectively $x_i \bar{v}_r$ and $y_i \bar{v}_r$, $i = 0, \dots, 3$. v_q denotes the tangent half of one of the revolute joints of the left 3R-chain and may therefore be one of the numbers 1, 2, 3 depending on the structure of the 3R-chain. \bar{v}_r denotes the tangent half of one of the revolute joints of the right 3R-chain and may therefore be one of the numbers 4, 5, 6 depending on the structure of the 3R-chain. Eq. (4) of S_6^2 is bilinear in x_i and y_i , $i = 0, \dots, 3$.

The solution algorithm of this intersection problem is straight forward. At first one normalizes the Study parameters by setting one suitable coordinate, say x_0 equal to one (at least one has to be non zero!). The remaining seven Study parameters are solved linearly from seven arbitrary hyperplane equations, say H_1, \dots, H_7 .

Remark 7. *It should be mentioned here that it is possible to solve the set of linear equations in full generality, that means without setting the DH parameters. But the output of the solution is that big that it does not make sense to operate with this solution. It is much faster to substitute the DH-parameters before solving the linear system.*

Multiplying the solutions for the Study parameters by the common denominator yields all Study parameters depending on the two parameters v_q and \bar{v}_r :

$$x_i = x_i(v_q, \bar{v}_r), \quad y_i = y_i(v_q, \bar{v}_r). \quad (28)$$

Substituting these Study parameters into Eq. (4) and in the one remaining equation H_8 one obtains two non-linear algebraic equations $E_1 = 0$ and $E_2 = 0$ in the two parameters: $E_1(v_q, \bar{v}_r) = 0, E_2(v_q, \bar{v}_r) = 0$.

Remark 8. *The vanishing of E_2 is the condition for intersecting the two one parameter sets of three spaces $T_c(v_q)$ and $T(\bar{v}_r)$ of SM_L and SM_R described by H_1, \dots, H_4 and H_5, \dots, H_8 . Hence, it can be also written as the determinant*

$$|\mathbf{h}_1, \mathbf{h}_2, \mathbf{h}_3, \mathbf{h}_4, \mathbf{h}_5, \mathbf{h}_6, \mathbf{h}_7, \mathbf{h}_8| = 0 \quad (29)$$

where \mathbf{h}_i are the hyperplane coordinates of H_i for $i = 1, \dots, 8$.

The resultant of E_1 and E_2 with respect to one unknown, e.g. \bar{v}_r , yields a univariate polynomial of degree 56 in the remaining unknown v_q . This polynomial factors into

$$(1 + v_q^2)^4 \mathcal{P}_1(v_q) \mathcal{P}_2(v_q) \mathcal{P}_3(v_q)^2 \mathcal{P}(v_q) = 0.$$

$(1 + v_q^2)$ yields the solutions $v_q = \pm I$, which belong to points in the exceptional generator and can be therefore canceled. The polynomials \mathcal{P}_1 and \mathcal{P}_2 are of degree four in v_q and belong, after back substitution of the roots and comparing the common roots of E_1 and E_2 to solutions $\bar{v}_r = \pm I$. Therefore also these two polynomials can be canceled. \mathcal{P}_3 is a polynomial of degree 12 and belongs to values of v_q that yield, back substituted into the solved linear system, solutions of the form $(0 : 0 : 0 : 0 : 0 : 0 : 0 : 0)$. This point is excluded from P^7 and therefore also \mathcal{P}_3 can be omitted from this polynomial. \mathcal{P} is the univariate polynomial of degree 16.

Remark 9. *The resultant factors in the described way in the general case. In special cases the factorization may look different, but the factors which do not solve the whole system can always be excluded with the same statements.*

Remark 10. *For every design it is possible to compute the univariate polynomial in a short time exactly. It depends on the degree of the polynomial if the roots can be obtained in closed form or only numerical.*

Solving \mathcal{P} for the unknown v_q yields 16 roots over \mathbb{C} . The other unknowns can be

computed by back substitution of these solutions into E_1 and E_2 . Solving both equations and comparing the solutions yields one common solution of the system for \bar{v}_r . Note that the solution of these unknowns are already the tangents half of two of the joint angles of the $6R$ -mechanism. Having the values of these two unknowns one can substitute the 16 pairs of solutions into the Study parameters that resulted from the solutions of the linear system in Eq. (28). This yields 16 poses where the right and the left coordinate systems coincide ($\Sigma_L = \Sigma_R$).

The remaining task is simple: One has to compute the inverse kinematics of two $2R$ -chains. To do this one has to compare the entries of the matrices describing the motion of the remaining $2R$ -chains $\mathbf{T}_1(u_1, u_2, u_3)$ (where one of the joint variables is fixed) in Eq. (25) and $\mathbf{T}_2(u_4, u_5, u_6)$ (where one of the joint variables is fixed) in Eq. (26), with the entries of the matrix that describe the pose of $\Sigma_L = \Sigma_R$. This leads to an overdetermined set of equations for the four unknown angles.

Theorem 1 gives another possibility to solve the inverse kinematics of the remaining $2R$ -chains. For every $3R$ -chain one has three different Segre manifolds to obtain the constraint manifold. For the derivation of the poses where $\Sigma_L = \Sigma_R$ we have used only one of them. The computed solutions have to be on all Segre manifolds. Using this fact one can obtain linear equations in the remaining four unknowns from the remaining four Segre manifolds.

Overconstrained 6R-Mechanisms In case that E_1 or E_2 vanish or the resultant of E_1 and E_2 vanishes we cannot create a univariate polynomial in one of the remaining unknowns. The $6R$ -chain is overconstrained. The remaining equation or the common factor determines the one parameter motion of the chain (see Pfulner-Husty[23]).

3 Synthesis of Mechanisms

Kinematic mapping can also be used in the synthesis of mechanisms. A detailed introduction into this interesting topic can be found in [19]. The mathematical tools used there are closely related to the presented methods within this paper. But there is a difference in the geometric interpretation of the devised equations. We show the application of our methods in the synthesis of a Bennett mechanism.

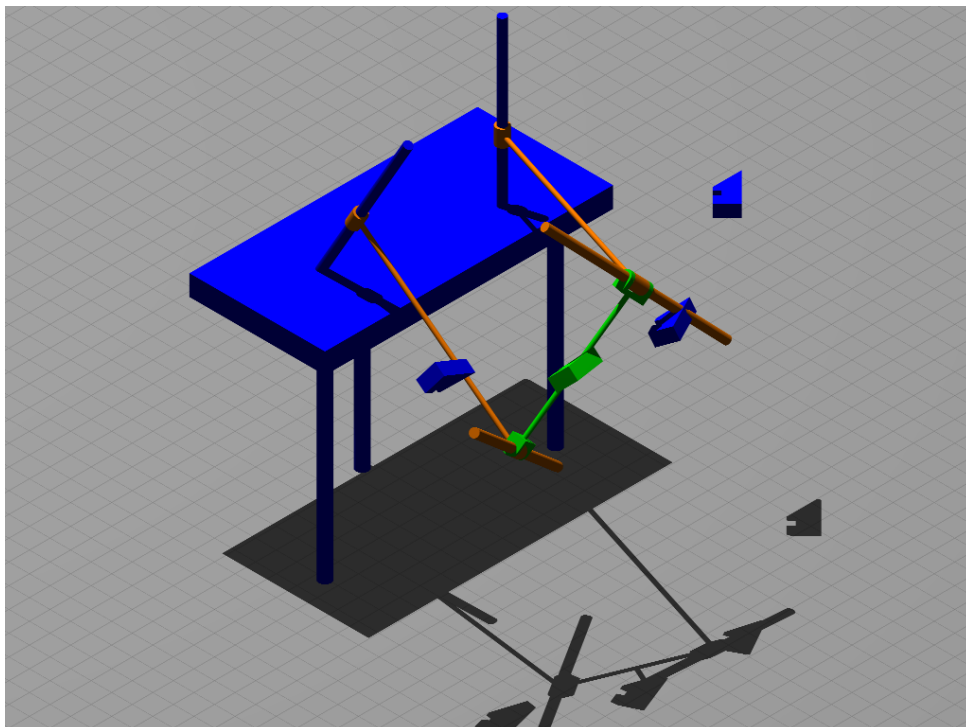


Figure 9: Bennett mechanism

The Bennett mechanism is a closed $4R$ -chain. It is well known that a Bennett mechanism can be synthesized exactly when three poses of the end effector system are given (Fig.9). Synthesis means that we have to find the design parameters of the mechanism and the location of the axes in the fixed system and the location of the moving body in the moving system. For the synthesis of such a mechanism we attach two of the revolute axes to the fixed system and two axes to the moving (coupler) system. Now we prize open the coupler link and obtain two open $2R$ -chains. The basic idea of the synthesis

is now: We map the possible displacements of the first $2R$ -chain onto S_6^2 . This yields the constraint manifold \mathcal{M}_1 of the $2R$ -chain in the kinematic image space. The same procedure we perform with the other $2R$ -chain and obtain a second constraint manifold \mathcal{M}_2 . Possible assembly modes of the two $2R$ -chains correspond to intersection points of \mathcal{M}_1 and \mathcal{M}_2 .

Due to the fact that a Bennett mechanism consists of two $2R$ -chains, one has to intersect two 3-spaces L_1^3, L_2^3 in P^7 . According to the well known dimension formula

$$\dim(U \cap V) = \dim(U) + \dim(V) - \dim(U + V) \quad (30)$$

where U, V denote sub-spaces of an n -dimensional space P^n , the intersection of two 3-spaces L_1^3, L_2^3 in a seven dimensional space P^7 can be:

- $\dim(L_1^3 \cap L_2^3) = -1, \Rightarrow$ intersection is empty,
- $\dim(L_1^3 \cap L_2^3) = 0, \Rightarrow$ intersection is one point,
- $\dim(L_1^3 \cap L_2^3) = 1, \Rightarrow$ intersection is a line,
- $\dim(L_1^3 \cap L_2^3) = 2, \Rightarrow$ intersection is a two-plane
- $\dim(L_1^3 \cap L_2^3) = 3 \Rightarrow L_1^3$ and L_2^3 coincide.

The first case is the general case. The mechanical interpretation is that two general $2R$ -chains never can be assembled to form a closed $4R$ -mechanism. There have to be conditions to make this happen. When the constraint manifolds are chosen such that they come from a $4R$ -chain, then they have exactly one point in common, which is on S_6^2 (forward kinematics of a serial $4R$ -chain). This fact is also a simple proof that the inverse kinematics of a general $4R$ serial chain has one solution. The case of the line intersection is only possible for special $4R$ -chains for which the inverse kinematics then has two solutions, which correspond to the two intersections of the line with S_6^2 . As we know, the Bennett motion is a one-parameter-motion, represented by a curve in the

kinematic image space. Therefore only the cases of a line, which lies completely on S_6^2 or a two-plane are of interest. The case that the line is contained in S_6^2 is not possible. Following Baker [2], who argued via screws, the relative motion between opposite links of a proper Bennett loop can be neither purely rotational nor purely translational at any time. Since straight lines on S_6^2 correspond to rotations or translations we can restrict ourselves to the case of $\dim(L_1^3 \cap L_2^3) = 2$. The kinematic image of the Bennett motion is therefore the intersection of a two-plane with the Study-quadric S_6^2 . This yields another confirmation of the fact that the synthesis of a Bennett needs three precision points. Three precision points correspond to three points on the Study-quadric and span the two-plane. This agrees with [26]. Summarizing we have:

Theorem 5. *Bennett motions are represented by planar sections of the Study-quadric and vice versa.*

The intersection of the two-plane and S_6^2 is a quadratic curve. In this sense Bennett motions can be regarded as the simplest non-trivial one parameter space motions. A direct consequence of the above considerations is the following

Corollary 2. *Bennett linkages are the only movable 4R-chains.*

It should be noted that to the authors' best knowledge up to now there exist only complicated algebraic proofs of this result (see for example [18]).

Synthesis algorithm Given are three precision points $A, B, C \in S_6^2$, corresponding to three poses of a coordinate system. The goal is to compute the design parameters of the Bennett mechanism that guides the coupler system through these poses. The above mentioned theorem states that the Bennett motion corresponds to the conic on S_6^2 passing through A, B and C . This conic can be parameterized rationally according to

$$\mathbf{f}(s) = \mathbf{p}_0 + s\mathbf{p}_1 + s^2\mathbf{p}_2, \quad \mathbf{p}_0, \mathbf{p}_1, \mathbf{p}_2 \in \mathbb{R}^8.$$

Applying inverse kinematic mapping by substituting the components of the vector function $\mathbf{f}(s)$ into Eq. (2) yields a rational parameterization $\mathbf{M}(s)$ of the Bennett motion. The trajectory of a point having homogeneous coordinates $(1, x_1, x_2, x_3)^T$ is the rational quartic

$$\mathbf{c}(s) := (X_0, X_1, X_2, X_3)^T(s) = \mathbf{M}(s)(1, x_1, x_2, x_3)^T. \quad (31)$$

After this step of the algorithm the motion of the coupler system of the synthesized Bennett mechanism is determined. For the mechanical design the axes and the Denavit-Hartenberg-parameters of the mechanism are necessary. To compute the parametric representation of the axes we follow the procedure developed in Bottema-Roth [6] in a slightly modified and adapted way. This is necessary because the motion is not given in the canonical form on which the geometric arguments in Bottema-Roth [6] are based. In Bottema-Roth [6] it is shown that there exist two pairs of conjugate complex isotropic planes $\psi_i, \overline{\psi}_i$ ($i = 1, 2$) whose points have trajectories of degree three or lower. Their pairwise intersections consist of four complex and two real lines. The two real lines are the moving axes of the Bennett mechanism and the paths of points on these lines are circles. The circles are in parallel planes having centers on common axes, the two real circle axes are the fixed axes of the mechanism. From Eq. (31) it is known that all trajectories $\mathbf{c}(s)$ are parameterized with rational functions of degree four. This is also true for the cubic trajectories and the circles. The only possibility to obtain a rational parametrization of degree four for twisted cubics is degree elevation of a rational cubic parametrization. Therefore in case of a cubic trajectory the parametric representation can be written in the form

$$\mathbf{c}(s) = (s - \tilde{s})\tilde{\mathbf{c}}(s) \quad (32)$$

where $\tilde{s} \in \mathbb{R}$ is constant and $\tilde{\mathbf{c}}(s)$ consists of cubic polynomials. We have to determine points in the moving system such that they have common zeros of all of their coordinate functions. As we know from above the solutions will be the points in the planes ψ_i and $\overline{\psi}_i$.

Since the homogenizing coordinate $X_0(s)$ is independent of x_1 , x_2 and x_3 , we can compute the zeros of this function. It turns out that the four zeros are pairwise conjugate complex s_1, \bar{s}_1, s_2 and \bar{s}_2 . The equations of the isotropic planes are found by substituting s_i and \bar{s}_i in either $X_1(s)$, $X_2(s)$ or $X_3(s)$. The computation of the mechanism's fixed and moving axes is now elementary. The implementation of this algorithm is straightforward. The most expensive step is solving the quartic equation $X_0(s) = 0$. As opposed to previous solutions no system of equations has to be solved and no discussion of reality of roots is necessary.

A second possibility to determine the axes is to compute the points which have planar trajectories because these points are on the moving axes. If the trajectory of a certain point is planar, the torsion of the trajectory has to vanish for all parameter values t . Following Husty et al. [13], the torsion is given by

$$\tau := \frac{\left| \frac{d\mathbf{c}(t)}{dt}, \frac{d^2\mathbf{c}(t)}{dt^2}, \frac{d^3\mathbf{c}(t)}{dt^3} \right|}{\left| \frac{d\mathbf{c}(t)}{dt} \times \frac{d^2\mathbf{c}(t)}{dt^2} \right|^2}.$$

$\tau = 0$ means that

$$\frac{d\mathbf{c}(t)}{dt}, \frac{d^2\mathbf{c}(t)}{dt^2}, \frac{d^3\mathbf{c}(t)}{dt^3}$$

have to be linearly dependent. Therefore the numerator of the determinant which is a function in t of degree 4 has to vanish identically for points on the moving axes. That means that all five coefficients of this polynomial have to vanish. Each coefficient is a cubic polynomial in the coordinates (x_1, x_2, x_3) of the moving point. This gives a system of five equations $F = [G_0, \dots, G_4]$ which is solvable but has no finite number of solutions, exactly as we expect.

For F a Gröbner basis can be determined. It turns out that the Gröbner basis contains only four polynomials $A = [B_0, \dots, B_3]$. The moving axes belong to the zero-set of A which is determined with help of resultants. Every possible resultant yields a polynomial

of degree nine which factors in a polynomial of degree three and one of degree six. The geometric interpretation of this fact is the following: The zeros of each of the the cubic polynomials determine a cubic surface in the moving space. These cubic surfaces have six lines in common and pairwise different three points. Two of the six lines are real. The axes in the fixed space can be computed vial the centers of the paths of the moving axes. For a numerical example we have to refer to Brunthaler [8, 7].

4 Conclusion

In this overview we have discussed the application of kinematic mapping and the resulting geometric-algebraic approach to solve problems in mechanism analysis and synthesis. It was shown that geometric preprocessing in a multidimensional setting allowed to simplify and subsequently solve the sets of polynomial equations linked to the mechanical problems.

References

- [1] Angeles, J., Fundamentals of Robotic Mechanical Systems. Theory, Methods and Algorithms, Springer, New York, 1997.
- [2] Baker, J. E. 1998. On the motion geometry of the Bennett linkage. Proceedings of the 8th International Conference on Engineering Computer Graphics and Descriptive Geometry. Austin. Texas. USA. pp. 433–437.
- [3] Bennett, G. T. 1903. A new mechanism. Engineering. Vol. 76. pp. 777–778.
- [4] Bennett, G. T. 1913–1914. The scew isogram-mechanism. Proceedings of the London Mathematical Society. Vol. 13. pp. 151–173.
- [5] Blaschke, W. 1960, *Kinematik und Quaternionen*, Wolfenbüttler Verlagsanstalt.
- [6] Bottema, O., Roth, B., 1990, *Theoretical Kinematics*, Dover Publishing.

- [7] Brunnthaler, K., Schröcker, H.-P., Husty, M. L., A new method for the synthesis of Bennett mechanisms, in: Proceedings of CK 2005, Cassino, Italy, 2005.
- [8] Brunnthaler, K., Synthesis of 4R Linkages Using Kinematic Mapping, PhD. thesis, Innsbruck, 2007.
- [9] Dickenstein, A. Emiris, I.Z., Solving Polynomial Equations, Foundations, Algorithms and Applications, Springer Pub., 2005.
- [10] Giering, O. *Vorlesungen über höhere Geometrie*, Vieweg Verlag, Braunschweig, 1983.
- [11] Harris, J. , Algebraic Geometry: A First Course, Vol. 133 of Graduate Texts in Mathematics, Springer, 1995.
- [12] Husty, M. L., 1996, "An Algorithm for Solving the Direct Kinematic of General Stewart-Gough Platforms", *Mechanism and Machine Theory*, vol. 31, No. 4, pp. 365-380.
- [13] Husty, M. L., Karger A., Sachs H., Steinhilper W., Kinematik und Robotik, Springer-Verlag, Berlin, Heidelberg, New York, 1997.
- [14] Husty, M.L., and Karger, A., 2000 "Self-Motions of Griffis-Duffy Type Platforms", *Proceedings of IEEE conference on Robotics and Automation (ICRA 2000)*, San Francisco, 7–12.
- [15] Husty, M. - Karger, A.: Self motions of Stewart-Gough platforms, an overview. Proceedings of the workshop on fundamental issues and future research directions for parallel mechanisms and manipulators, Quebec City, 131 –141, (2002).
- [16] Husty, M. L. - Pfulner, M. - Schröcker, H.P., A New and Efficient Algorithm for the Inverse kinematics of a General 6R, Proceedings of IDETEC/CIE 2005, DETEC/MECH-84745, 2005, 8p.

- [17] Husty, M. L. - Pfulner, M. - Schröcker, H.P., A New and Efficient Algorithm for the Inverse Kinematics of a General 6R, Mech. Mach. Theory, 2007.
- [18] Karger, A. 4-parametric robot-manipulators and the Bennett's mechanism. Private communication.
- [19] McCarthy J.M., Geometric Design of Linkages, Vol. 320 of Interdisciplinary Applied Mathematics, Springer-Verlag, New York, 2000.
- [20] Merlet, J.P., 2000, *Parallel Robots*, Kluwer Academic Publishers, Dordrecht, The Netherlands.
- [21] Naas J., Schmid H., Mathematisches Wörterbuch, Vol. Band II, Akademie-Verlag Berlin, 1974.
- [22] Pfulner, M., Analysis of spatial serial manipulators using kinematic mapping, PhD. thesis, Innsbruck 2006 .
- [23] Pfulner, M. - Husty M., Determining the motion of overconstrained 6R mechanisms, Proceedings of IFToMM world congress, Besancon, 2007, accepted for publication.
- [24] Selig, J. M., Geometric Fundamentals of Robotics, Monographs in Computer Science, Springer, New York, 2005.
- [25] Study E., Geometrie der Dynamen, B. G. Teubner, Leipzig, 1903.
- [26] Suh, C. H., Radcliffe, C. W. 1978. Kinematics and Mechanisms Design. John Wiley and Sons. Canada.
- [27] Sommese, A, Verschelde, Wampler, Ch., 2002, "Advances in Polynomial Continuation for Solving problems in Kinematics", preprint.